A THESIS SUBMITTED TO
THE GRADUATE SCHOOL OF NATURAL AND APPLIED SCIENCES
OF ÇANKIRI KARATEKİN UNIVERSITY

INVESTIGATION OF THE INTERACTION OF THE MOLECULAR STRUCTURE OF COMPOUND $C_{24}H_{24}N_6OS_2$ WITH DNA BASES BY DFT

IN PARTIAL FULFILLMENT OF THE REQUIREMENTS
FOR
THE DEGREE OF MASTER OF SCIENCE
IN
PHYSICS

BY

ZAINULABDEEN MOHAMMED JALIL JALIL

ÇANKIRI

2023

INVESTIGATION OF THE INTERACTION OF THE MOLECULAR STRUCTURE OF COMPOUND $C_{24}H_{24}N_6OS_2$ WITH DNA BASES BY DFT

By Zainulabdeen Mohammed Jalil JALIL

June 2023

We certify that we have read this thesis and that in our opinion it is fully adequate, in scope and in quality, as a thesis for the degree of Master of Science

Advisor **:** Prof. Dr. Çiğdem YÜKSEKTEPE ATAOL

Examining Committee Members:

Chairman **:** Prof. Dr. Çiğdem YÜKSEKTEPE ATAOL
Physics
Çankırı Karatekin University

Member **:** Prof. Dr. Hamit ALYAR
Physics
Çankırı Karatekin University

Member **:** Prof. Dr. Sibel DEMİR KANMAZALP
Technical Sciences, Biomedical Device Technology
Gaziantep University

Approved for the Graduate School of Natural and Applied Sciences

Prof. Dr. Hamit ALYAR
Director of Graduate School

I hereby declare that all information in this document has been obtained and presented in accordance with academic rules and ethical conduct. I also declare that, as required by these rules and conduct, I have fully cited and referenced all material and results that are not original to this work.

Zainulabdeen Mohammed Jalil JALIL

ABSTRACT

INVESTIGATION OF THE INTERACTION OF THE MOLECULAR STRUCTURE OF COMPOUND $C_{24}H_{24}N_6OS_2$ WITH DNA BASES BY DFT

Zainulabdeen Mohammed Jalil JALIL

Master of Science in Physics

Advisor: Prof. Dr. Çiğdem YÜKSEKTEPE ATAOL

June 2023

The molecular structure of a chemical compound consisting of tetrazole, thiazole, cyclobutane, acetamide, and phenyl rings was investigated using Density Functional Theory (DFT), one of the computational chemistry methods. In the calculations, the B3LYP basis function and the split valence and polarized split valence basis sets of 6-311G and 6-311G(d, p), respectively, were used. The molecular structure of the compound with the closed formula $C_{24}H_{24}N_6OS_2$ was optimized in both ethanol and water environments, and bond parameters were obtained. By using optimized molecular structures, a single-point energy calculation was made in the ground state in water and ethanol environments. After obtaining the most stable structure of the molecular structure corresponding to the lowest energy, the molecular electrostatic potential map was obtained, the Fukui functions were calculated from the natural population analysis charges, and the molecular orbital energy values were obtained. The reactivity parameters of the molecular structure were formed from the molecular orbital energy values and the charge transfer parameters were derived, and the interaction between DNA bases such as adenine, guanine, cytosine, and thymine and the molecular structure was investigated.

2023, 42 pages

Keywords: Density functional theory, DNA bases, Molecular orbital energy, Reactivity parameters

ÖZET

$C_{24}H_{24}N_6OS_2$ BİLEŞİĞİNİN MOLEKÜLER YAPISININ DNA BAZLARI İLE ETKİLEŞİMİNİN DFT İLE ARAŞTIRILMASI

Zainulabdeen Mohammed Jalil JALIL
Fizik, Yüksek Lisans
Tez Danışmanı: Prof. Dr. Çiğdem YÜKSEKTEPE ATAOL
Haziran 2023

Tetrazol, tiyazol, siklobütan, asetamid ve fenil halkalarından oluşan bir kimyasal bileşiğin moleküler yapısı hesaplamalı kimya yöntemlerinden biri olan Yoğunluk Fonksiyonel Teorisi (YFT) kullanılarak araştırılmıştır. Hesaplamalarda hibrit fonksiyonlardan B3LYP baz fonksiyonu ile 6-311G ve 6-311G(d, p) sırasıyla split valans ve polarize split valans baz setleri kullanılmıştır. Kapalı formülü $C_{24}H_{24}N_6OS_2$ olan bileşiğin moleküler yapısı hem etanol hem de su ortamlarında optimize edilerek bağ parametreleri elde edilmiştir. Optimize edilmiş moleküler yapılar kullanılarak taban durumda su ve etanol ortamlarında tek nokta enerji hesabı yaptırılmıştır. Moleküler yapının en düşük enerjiye karşılık gelen en kararlı yapısı elde edildikten sonra moleküler elektrostatik potansiyel haritası elde edilmiş, doğal popülasyon analiz yüklerinden Fukui fonksiyonları hesaplatılmış ve moleküler orbital enerji değerleri elde edilmiştir. Moleküler orbital enerji değerlerinden moleküler yapının reaktivite parametreleri oluşturulmuş ve yük transfer parametreleri türetilerek adenin, guanin, sitozin ve timin gibi DNA bazları ile moleküler yapı arasındaki etkileşim araştırılmıştır.

2023, 42 sayfa

Anahtar Kelimeler: Yoğunluk fonksiyonel teorisi, DNA bazları, Moleküler orbital enerji, Reaktivite parametreleri

PREFACE AND ACKNOWLEDGEMENTS

I would like to thank my thesis advisor, Prof. Dr. Çiğdem YÜKSEKTEPE ATAOL, for her patience, guidance and understanding.

Zainulabdeen Mohammed Jalil JALIL

Çankırı-2023

CONTENTS

LIST OF SYMBOLS

a.u.	Atomic unit
a_0	Bohr radius
ΔN	Charge transfer
η	Chemical hardness
μ_X	Chemical potential
ε	Dielectric constant
μ	Dipole moment
$\rho(r)$	Electron density
χ	Electronegativity
ω	Electrophilicity index
ΔE	Energy gap
E_{HOMO}	Energy level of HOMO
E_{LUMO}	Energy level of LUMO
f_k	Fukui function
S	Global softness

LIST OF ABBREVIATIONS

A	Adenine
C	Cytosine
DFT	Density functional theory
DNA	Deoxyribonucleic acid
EA	Electron affinity
ECT	Electrophilicity-based charge transfer
G	Guanine
GTOs	Gaussian type orbital
HOMO	Highest molecular orbital
IP	Ionization potential
LUMO	Lowest molecular orbital
MEP	Molecular electrostatic potential
MM	Molecular mechanics
NPA	Natural population analyses
SE	Semi-empirical
STOs	Slater type orbital
T	Thymine
UV	Ultraviolet

LIST OF FIGURES

LIST OF TABLES

1. INTRODUCTION

Four basic techniques are available to computational chemists and doctors: ab initio, Density Functional Theory (DFT), Semi-Empirical (SE), and Molecular Mechanics (MM) (Andreoni and Curioni 2002). The foundation of today's computational atomic, molecular, solid state, and even nuclear physics are density functional approaches, which are diverse and extremely active. These techniques are widely used by computational physicists because of their great effectiveness. The Hohenberg-Kohn theory, the Thomas-Fermi theory, and density functional notions all entered the realm of mathematical physics in the 1970s and 1980s, respectively. The physical properties of substances, molecular geometries, molecule energies, chemical reactivity, IR, UV, and NMR spectra are among the topics that computational chemistry frequently studies (Eschrig 1996).

The Density Functional Theory (DFT) methodology is becoming used by more researchers. DFT is the most widely utilized quantum mechanical modeling technique for analyzing the electronic, magnetic, structural, and vibrational features of materials because it is strong, adaptable, and successful. It was developed by Hohenberg, Kohn, and Sham to describe the electronic charge density in terms of the ground state characteristics of many-electron systems. By using non-interacting electrons moving in an effective potential to solve the problem, the many body difficulties associated with interacting electrons in a static external potential are minimized (Yong 2001).

The molecular structure of the compound with the closed formula $C_{24}H_{24}N_6OS_2$ has been elucidated using Density functional theory (DFT) from computational chemistry methods. The $C_{24}H_{24}N_6OS_2$ was optimized in water and ethanol solvent environments and the stable structure corresponding to the lowest energy was obtained. The molecular electrostatic potential (MEP) surface was obtained in water and Fukui functions were obtained and reactivity parameters were found and its interaction with Deoxyribonucleic acid (DNA) bases was investigated.

2. LITERATURE REVIEW

In this section, brief information is given about the tetrazole, thiazole, acetamide, and cyclobutane groups that constitute the functional groups of the $C_{24}H_{24}N_6OS_2$.

2.1 Tetrazoles

Tetrazoles are aromatic five-membered rings with one carbon and four nitrogen atoms that are twice unsaturated. They do not exist in nature. Pentazoles have the most nitrogen atoms of any stable heterocycle (Neochoritis *et al.* 2019) because they are highly explosive even at low temperatures. Bladin (1885), a Swedish chemist, published the primary report on the synthesis of a tetrazole derived at Upsala University. He discovered that the response of dicyanophenylhy-drazine and nitrous acid created a compound, for which he later proposed the name "tetrazole". Based on the number of substituents, tetrazoles are characterized as unmono-, di-, or trisubstituted. 5-Substituted tetrazoles with 6 electrons can be I or II tautomeric (Figure 2.1). The 1H tautomer is more stable in solution however, the 2H tautomer is more stable in gas (Bhatt 2011).

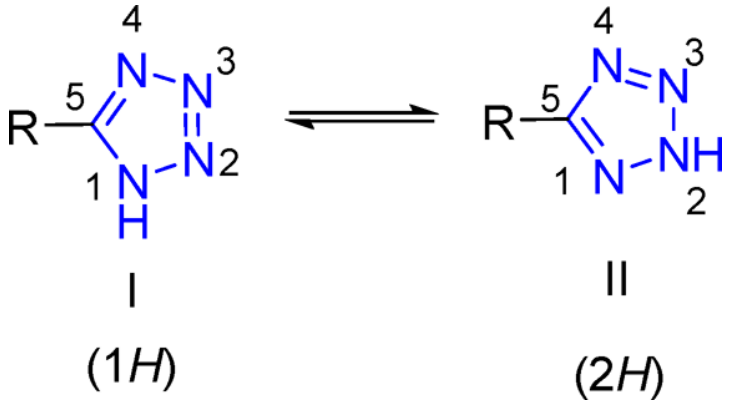

Figure 2.1 Tautomersim of tetrazole derivatives (Bhatt 2011)

The tetrazole element is an essential chemical scaffold that has discovered widespread uses in healthcare, biochemistry, and industry as materials, such as those used in photography, imaging chemicals, and military applications (Bladin 1885). Tetrazole derivatives are being researched as latent explosives and rocket propellent components

due to their high energy characteristics. The high nitrogen content of tetrazoles suggests that they could be used as a sustainable component of gas generators with an excellent combustion rate and high stability. However, tetrazoles' most essential and beneficial utilization, with various potential applications, is in biomedical sciences (Benson 1947).

2.2 Cyclobutane

Cyclobutane was first produced in 1907. No biological qualities, odorless, colorless gas. Cyclobutane rings are rare but found in natural products, mostly from marine and plant species (Willstätter and Bruce 1907). Agelas spectrum sceptrins' antibacterial activities were greatly enhanced by their cyclobutane skeletal structure (1) (Figure 2.2) (Wang and Lippard 2005). In addition, when exposed to ultraviolet (UV) rays, DNA bases can [2+2] photo dimerize and establish cyclobutane pyrimidine dimers (2) (Figure 2.2). Such DNA adhesion may result in a variety of negative consequences, including skin cancer. Although cyclobutane rings had also lately been incorporated into pharmaceutically active compounds, inorganic-based cyclobutane medicines were utilized for many ways too long, most noticeably in a medication that creates cancer cells to die by crosslinking DNA. Carboplatin (3) is a chemotherapy drug that is frequently employed for treating advanced tumors including ovarian, testicular, cervical, head, and neck cancers (Wang and Lippard 2005, Lazarević *et al.* 2017).

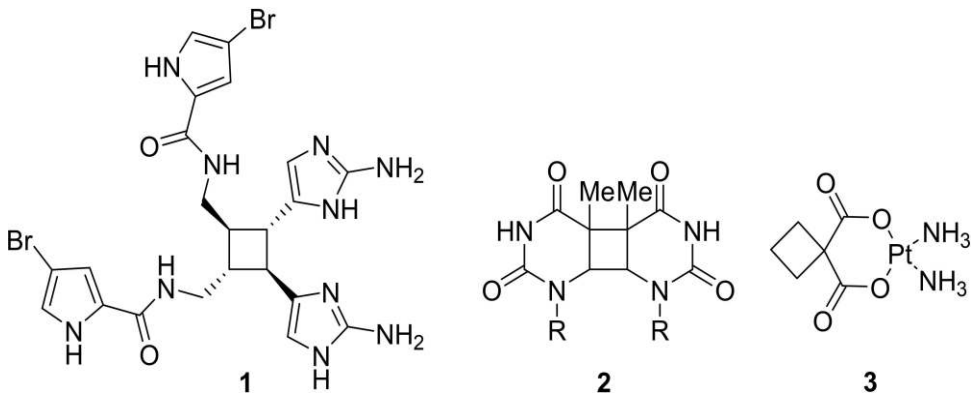

Figure 2.2 Agelas spectrum sea sponge cyclobutane (1), thymine dimer (2) (R denotes the rest of the DNA helix), and carboplatin (3) (Wang and Lippard 2005)

Cyclobutanes are being employed more frequently in medicinal chemistry for target validation. In comparison to other carbocycles, the cyclobutane ring is unusually chemically inert due to its puckered structure, longer C-C bond lengths, greater C-C character, and high strain (Van Der Kolk *et al.* 2022).

Due to their use in both synthetic and biological processes, tiny molecules containing heterocyclic rings integrated with nitrogen and sulfur, such as thiazole and triazole, have been the subject of intense investigation throughout the years (Ripain and Ngah 2021). The most frequently mentioned chemical in the literature is thiazole. Thiazole is a 5-membered ring moiety with nitrogen and sulfur, respectively, at positions 1 and 3 (Yurttaş *et al.* 2015, Floros *et al.* 2016). Thiazole derivatives are largely concerned with the structural pattern of replacing hydrogen atoms in positions 2, 4, and 5 with desired moieties as active compounds. It has been reported that the chemicals have characteristics against inflammation, fungus, cancer, bacteria, convulsions, viruses, and tumors (Al-Saadi *et al.* 2008, Zamigajlo *et al.* 2013, El-Sayed *et al.* 2009, Siddiqui *et al.* 2009, Hassan 2012, Nalawade *et al.* 2013, Cai *et al.* 2016).

2.3 Thiazole

Thiazole is an unchanging heterocyclic compound that contains both an electron-donating (-S-) and an electron-accepting (C=N) group. Thiazole and its analogs, like oxazole, are believed to belong to a significant class of heterocycles with a wide range of biological properties (Gupta and Kant 2013). Thiazole is isomeric with isothiazole, an azole compound with similar atoms (nitrogen and sulfur) but in various positions. The boiling point of thiazole is between 116 and 118 degrees Celsius, and it is a transparent, pale-yellow liquid. It dissolves easily in ether and alcohol but just slightly in water. According to Huckel's rule, the thiazole heterocyclic ring contains a delocalization of 6 electrons from the lone pair electrons (Khan *et al.* 2016).

Thiazole has a unique molecular structure due to its versatile building blocks as bioactive compounds. Many studies have discovered the thiazole ring in a wide variety of biologically active natural and manufactured products. Vitamin B1, also known as

thiamine, is an exemplar of a thiazole moiety that naturally supports the nervous system through its role in acetylcholine fabrication (Gupta *et al.* 2013). Moreover, the amphiphilic properties of the thiazole derivative products seen in Figure 2.3 were attributed to the presence of both hydrophobic (lipophilic) and hydrophilic (lipophobic) parts. This feature improves its capacity to readily distribute into bacterial cell membranes for inhibition activity (Sauer *et al.* 2017, Rouf and Tanyeli 2015).

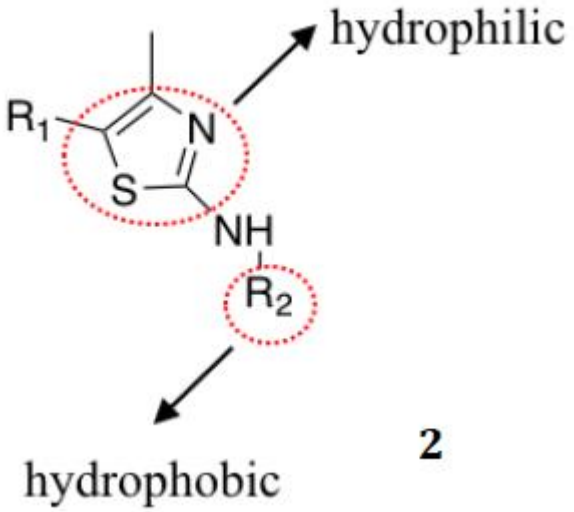

Figure 2.3 Structure of thiazole derivatives (Rouf and Tanyeli 2015)

2.4 Acetamide

Acetamide is a naturally occurring irritant; it is the sensible amide produced by acidic corrosives. The related compound N-dimethylacetamide is much more widely used, but it is not ready from acetamide, which would be worn as a systematic material, but it is also used in of a blend (Chauhan *et al.* 2020). Acetamide was first manufactured in France in 1986 and is currently available in Europe. America is considering the assistance of African sleep disorders. Modafinil was discovered in 1998. Acetamide, on the other hand, is an oral medication, and the intravenous equivalent can be a butt-centric suppository or an inward breath course from a sedate organization (Horton *et al.* 2003). Which is employed in specific situations. As subordinates to ten people. Have a dissolving operator

including such natural mixtures of inflammable balms with a hygroscopic professionals in mind.

The most obvious purpose of these subordinates is as a luxurious Sass pain reliever. It is a case of pain-relieving operators (Kasai *et al.* 2001) because it has defused Paracetamol, one of the world's greatest commonly used medications. It is also claimed that acetamide is responsible for antimicrobial cancer preclusion agent comforting training. Capable of practical gathering. The natural evaluation of the CNS operative act has been completed. It is built up such knowledge about all the makes three combinations appear active central sensory system delegate action out of the biologic thought. According to the writing, Acetamide has effects such as antimicrobial training, cancer preclusion agent exercises, and calming exercises. CNS operative, for example. They are highly critical in their organic activities and for their reactions to nucleophiles, which allows for the combination of a similarly large number of heterocycles. Acetamide has the atomic formula C_2H_5NO, according to Figure 2.4 (Rajasekaran and Murugesan 2005).

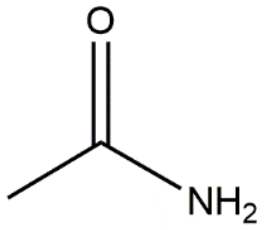

Figure 2.4 The chemical structure of Acetamide (Rajasekaran and Murugesan 2005)

2.5 Deoxyribonucleic acid (DNA)

The basic biochemical basis for the genetic code is provided by Watson-Crick base pair recognition, and knowledge of the genes that encode proteins as well as the genetic variations that cause dysfunction and disease has advanced dramatically (Booth *et al.* 2015) The main sequence of the DNA letters G, C, A, and T has been a major focus of research on DNA in living systems. Since the International Human Genome Project read the human reference genome, developments in DNA sequencing technology have made it possible to decipher the primary DNA code for the entire genomes of species, especially

humans, whose annual genome output is approaching the millions (Raiber *et al.* 2017). As just a result, there have been a significant variety of recent discoveries regarding the fundamental structure of genomes and how the function is related to them. These advancements have led to an explosion in the variety of genome-based applications in society, from testing for consumers (such as ancestry determination) to the description and control of diseases (such as cancers and rare genetic diseases) as a crucial part of individualized genomic medicine (Traube and Carell 2017). The importance of the DNA's primary sequence is evident, but other key parts of DNA have gotten less attention and, as a result, are less well-known. The goal of this perspective is to study how cells and other organisms' genomic DNA undergoes chemical changes. Understanding DNA alterations and how they impact DNA's structure and function has recently attracted more attention to comprehend their larger significance to the biology of animals in both healthy and diseased scenarios (Carell *et al.* 2018). For a very long time, people have been aware of certain alterations to bases, such as the epigenetic base 5-methylcytidine. This is not the case for many DNA base changes and the enzymes that add or remove them in mammalian DNA. As a result of this, scientists have devised brand new chemical approaches and procedures to locate particular chemical modifications within genomes. Such modifications, which are still occurring, are motivating studies to determine which chemically altered bases do critical roles and how the molecular processes that are behind them function (Luo *et al.* 2018).

Nucleic acids are made up of nucleotides, which are biopolymers. Latter has a sugar-phosphate backbone, a heterocyclic aromatic base, also called a nucleobase, a sugar with a five-atom ring, and a phosphate unit that connects the sugars. Figure 2.5 shows the shapes of the nucleobases, the two sugars, and the nucleobase-sugar bonds, which are also called nucleosides (Devine and Jheeta 2020).

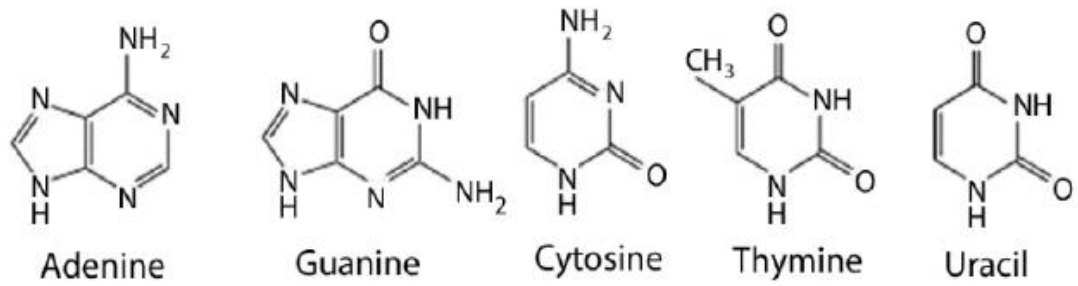

Figure 2.5 The chemical structure of deoxyribonucleic acid (DNA) bases (Devine and Jheeta 2020)

3. MATERIALS AND METHODS

The single crystal structure of the compound $C_{24}H_{24}N_6OS_2$ consisting of tetrazole, thiazole, and acetamide groups was previously elucidated by Örnek (2019). To investigate the properties of $C_{24}H_{24}N_6OS_2$ in this thesis, the atomic coordinates of this compound were taken from Örnek (2019) to save calculation time. This thesis contains only the results of theoretical calculations. All calculations of the molecular structure were performed with Gaussian 09 program (Frisch *et al.* 2009). Density functional theory, which gives very good results for organic compounds, was chosen for the calculation. To determine a molecule structure's overall energy level, the computations make use of functionals that take into consideration the exchange-correlation energy. In this study, the B3LYP basis function was chosen from hybrid functionals that include exchange energy (Becke 1993) and correlation energy (Lee *et al.* 1988) in the calculation. To construct the electron density function of the $C_{24}H_{24}N_6OS_2$, the wave functions of the atoms constituting the molecular structure are needed. In the calculations, split valence 6-311G and divide and conquer valence 6-311(d, p) basis sets were chosen as the basis sets that form the wave functions. The molecular structure, physical and chemical properties of $C_{24}H_{24}N_6OS_2$ have been previously investigated by different methods for gaseous media, but its molecular structure has not been investigated for different solvent media. In this study, the $C_{24}H_{24}N_6OS_2$ was optimized in water and ethanol solvent environments in the ground state. Using the optimized structures, single point energy calculation was performed and its stable structure in solvent environments was investigated. To understand whether it is nucleophilic or electrophilic in water, the molecular electrostatic potential map was obtained and Fukui functions were calculated. The interaction with DNA bases like adenine, guanine, cytosine, and thymine was studied, and global reactivity characteristics were generated from the computed molecular orbital energies.

3.1 Density Functional Theory (DFT)

One of the most popular and fruitful quantum mechanical approaches to computing the electronic structure of matter is density functional theory (Valone 2010). Functionally preceding density theory was the Thomas-Fermi model, developed by Thomas and Fermi

in 1927. You can see how the number of electrons in an atom affects its kinetic energy by drawing a graph, Thomas and Fermi were able to calculate the energy of an atom. Molecular structures, vibrational frequencies, ionization energies, electric and atomization energies, reaction pathways, and magnetic characteristics are just a few of the many molecular features that DFT can predict (Fitts 1999).

As a result of the much-decreased CPU time, DFT approaches are gaining popularity as the results are comparable to those achieved by employing ab initio methods. The DFT approach varies from other HF calculation-based methods in that it computes energy using the electron density rather than a wave function (Sholl and Steckel 2022).

DFT uses the electron density ρ(r) to determine a wide variety of particle characteristics. The electron density of a state is equal to the number of electrons per unit volume of that state (Bransden and Joachain 2003). The number of electrons in the system is irrelevant, as demonstrated in Equation (3.1); all that is required are three coordinates (Mueller 2007).

$$N = \int \rho(\vec{r})\, d\vec{r} \tag{3.1}$$

The probability of locating an electron (or electrons) in a given region decreases to zero as the distance from the nucleus increases to infinity. With additional electrons, the wavefunction approaches become theoretically much more difficult. All ground-state electrical characteristics are defined solely by electron density, and DFT uses ground-state energy as its starting point. In addition, the electrical density is well-matched to the system's precise ground state, resulting in low total energy (Kohanoff and Gidopoulos 2003).

3.2 Born-Oppenheimer Approximation

The Born-Oppenheimer assumption characterizes the separation of nucleon and electron movement in molecules. Molecules include both nuclei and electrons. It is possible to

split the overall wavefunction of a molecule into two parts: one component is responsible for the nuclear variables, while the other part is responsible for the electron variables, as in Equation (3.2) (Cramer 2013).

$$\Psi_{\text{total}} = \Psi_{\text{electron}} * \Psi_{\text{nucleus}} \tag{3.2}$$

Since nuclei are so much heavier than electrons, they move at much lower velocities than the latter. The difference between their masses is three to four orders of magnitude. It is possible to regard it as being fixed. Therefore, if the nuclei are immobile in space and do not change position, then the nuclei's kinetic energy is equal to zero, and the potential energy of nuclei-nuclei might be assumed to be constant. In addition to this, neither the second nor the final terms exist in Equation (3.2). Therefore, the Hamiltonian operator has only three terms as in Equation (3.3): electron kinetic energy ($\hat{\mathrm{T}}_e$), electron-electron interaction energy($\hat{V}_{ee}$), and electron-nuclear interaction energy ($\hat{V}_{ne}$).

$$\hat{H} = \hat{T}_e + \hat{V}_{ne} + \hat{V}_{ee} \tag{3.3}$$

All electrons move in a potential field of fixed nuclei. Thus, molecule total energy calculations are simplified and huge molecule wavefunction computations can be solved (Jensen 2017).

3.3 Thomas Fermi Dirac Theorem

The Thomas-Fermi theory was originally developed by Thomas and Fermi to explain the uniform distribution of electrons in the outer shell of a heavy atom. The Thomas-Fermi theory was developed for this reason. This model has been updated to account for correlation, exchange, quantum, and multi-shell effects more fully. When it comes to the self-consistent Hartree field equations, the semi-classical (WKB) limit is the Thomas-Fermi theory. The initial approximation nature of Thomas-Fermi's theory contains a dual nature. First, it's important to disregard the model's correlation effects, which show that the Hartree approach is inaccurate and that there is a consistent (on average) discrepancy

between the actual physical interaction and the model's predictions of that interaction. Second, in the Thomas-Fermi theory, the effects of quantum mechanics are ignored due to the semi-classical nature of the atomic description (Seriy 2015).

Pucci, R. and March 1982 note that Thomas (1926) and Fermi (1927) separately viewed the cloud of electrons surrounding an atomic nucleus as a degenerate electron gas. The Fermi momentum F(r) can be calculated as a function of the electronic density $\rho_F(r)$ at location r away from the nucleus, as in Equation (3.4)

$$\rho(r) = 2\ \frac{4\pi}{3} p_F^3(r) \tag{3.4}$$

In which the Pauli exclusion principle is taken into consideration by multiplying by a factor of 2. The Equation (3.5) relating the Fermi momentum pF(r) at location to the self-consistent potential V(r) (Pucci and Angilella 2006):

$$p_F^2\ (r) = 2m[E_F - V(r)] \tag{3.5}$$

where m represents the mass of an electron and E_F stands for the Fermi energy. The latter is attainable by the normalization criterion as in Equation (3.6) (Pucci and March 1982).

$$\int \rho(r) d^3r = N \tag{3.6}$$

In a neutral atom, the total number of electrons, denoted by N, is equal to the atomic number, Z. Inserting Equation (3.5) into Equation (3.4), Using the screening factor, and the Poisson equation for electrostatics, we can obtain Equation (3.6) (Pucci and March 1982).

$$V(r) - E_F = -\frac{Ze^2}{r}\ \phi(r) \tag{3.7}$$

Therefore, the dimensionless Thomas-Fermi equation for a spherically symmetric distribution of electrons can be derived as in Equation (3.8) (Pucci and March 1982)

$$\frac{d^2\phi}{dx^2} = \frac{\phi^{3/2}}{x^{1/2}} \tag{3.8}$$

where $r = bx$

and b is the scaling factor as in Equation (3.9)

$$b = \frac{1}{4}\left(\frac{9x^2}{2Z}\right)^{1/3} = \frac{0.8853}{Z^{1/3}}a_0 \tag{3.9}$$

with a_0 the Bohr radius

Equation (3.5) is "universal" since only the scaling factor b depends on the atomic number Z. In Thomas Fermi approximation, solving Equation (3.5) for one atom solves it for all others by scaling distance by b.

3.4 Basis Sets

Basis sets characterize atoms' orbitals. Linear combinations of basis functions and angular functions yield entire wave functions and molecular orbitals. Semiempirical methods use specified basis sets. Most calculations employ established basis sets. A basis set must be specified when performing ab initio or density functional theory calculations. The two main elements affecting the accuracy of outcomes are the type of calculation used and the basis set selected (Springborg 2000).

3.4.1 Slater-type orbitals (STOs)

It appears to be an obvious option for base functions. They are exponential and precisely imitate the hydrogen atom's eigenfunctions. Many-center integrals, including coulomb

and HF-exchange components, are challenging to compute using (STO), which is one of its drawbacks (STO). Thus, it is irrelevant to current wave function-based quantum chemical codes (Lipkowitz and Boyd 2008).

3.4.2 Gaussian-type orbitals (GTOs)

Because they are good at analytically calculating many-center integrals, HF and similar approaches use the (GTO) basis function. Enhancing GTO basis sets usually involves combining basic Gaussian functions to create a contracted Gaussian function (CGF) (Camargo *et al.* 2003). Nuclei's wave tail representation is inferior to the GTO's STO function. The same accuracy requires three times as many GTOs as STOs, according to a preliminary calculation. The Gaussian basis set has the advantage that two Gaussian functions yield another Gaussian function. Hence, the analytical solution for Gaussian functions computes Coulomb and HF-exchange terms. Minimum basis sets, split valence sets, polarisation, and diffuse functions, and others are Gaussian basis sets (Udhayakala and Rajendiran 2011).

3.4.2.1 Minimal basis sets

The minimal basis set describes a molecule's ground states and fully represents each atom's electrons with the fewest basis functions X. STO-nG is a minimum basis set with n Gaussian primitive functions (n=2-6). This basis sets share core and valence orbital Gaussian primitives. Minimal basis sets yield messy results inappropriate for research publication (Minkin 1999, Kampen *et al.* 1999).

3.4.2.2 Split-valence basis sets

Split-valence basic sets (Pople basis sets) depict valence orbitals with two or more basis functions and inner-shell atomic orbitals with one (Dorsett and White 2000). Add basis functions to orbitals to increase a basis set. Split-valence basis sets have one basis function for core orbitals and numerous for valence orbitals with various orbital exponents. VTZ

basis sets have three basic functions per valence orbital, unlike VDZ's two. Split valence basis sets better represent molecular orbitals since they support different atom sizes, but they cannot build their own balanced basis set (Gotwals and Sendlinger 2007).

3.4.2.3 Polarization and diffuse functions

The basis set must have polarization functions to enhance the findings. Higher angular momentum functions are polarization functions, which include p- and d-type functions for hydrogen and helium atoms and d- and f-type functions for heavier atoms (Reimers 2011). Allowing the orbital's shape to change, increases the base set's adaptability (i.e., become polarized in one direction). In systems containing hydrogens, such as hydrogen bonding and proton transfers, polarization functions are advantageous because they permit the s orbital to diverge from its typical spherical form. Since they yield more precise computed geometries and vibrational frequencies, polarization functions are widely used (Santos *et al.* 2005).

Following the same convention as the contraction method, we use brackets () to signify the addition of polarization functions and a plus sign (+) to denote the addition of diffuse functions. For instance, in the basis set 6-31++G (d, p), all heavy elements have d-type functions while hydrogen and helium have p-type ones. Indicated by the first "+," diffuse s- and p-type functions on heavy atoms are, and the second "+" indicates diffuse s-type functions on hydrogen (Kwon *et al.* 2004, Sherrill 2002).

3.5 Base Functions

Base functions serve as the building blocks for more complicated functions, which are referred to as derived features in machine learning. In other words, they are a collection of k common functions used to estimate a difficult or impossible to precisely model function.

For instance, a polynomial function can be created by connecting the powers of x of different individuals, such as the basis functions 1, x, x2, x3, etc. A basis set is the collection of fundamental functions that were used to build the more sophisticated function. The ideal situation is to use a set of as few functions as you can because it is feasible to manually develop numerous sophisticated functions. However, numerous real-world situations include thousands of basic functions, making a computer necessary (Ramsay and Silverman 2005).

The following base function types are the most typical (Svishcheva *et al.* 2015):

- Basis for polynomials: 1, x, x2, x3 —
- A collection of k polynomial functions, each of a specific order d, make up the B-Spline basis. The quantity of constants needed to define a function is called an order. For non-periodic data, popular.
- The sine and cosine functions of the Fourier basis are as follows: 1, sin(x), cos(x), sin(2x), cos(2x), sin(3x), cos(3x) & hekkip; they are frequently utilized to create periodic functions. Although these functions' derivatives are simple to calculate, they are not appropriate for representing discontinuous functions.

4. RESULTS AND DISCUSSION

The chemical diagram of the compound $C_{24}H_{24}N_6OS_2$, which was crystallized in ethanol media, found to have a molecular weight of 476.6 g and whose single crystal structure was previously elucidated by Örnek (2019), is given in Figure 4.1.

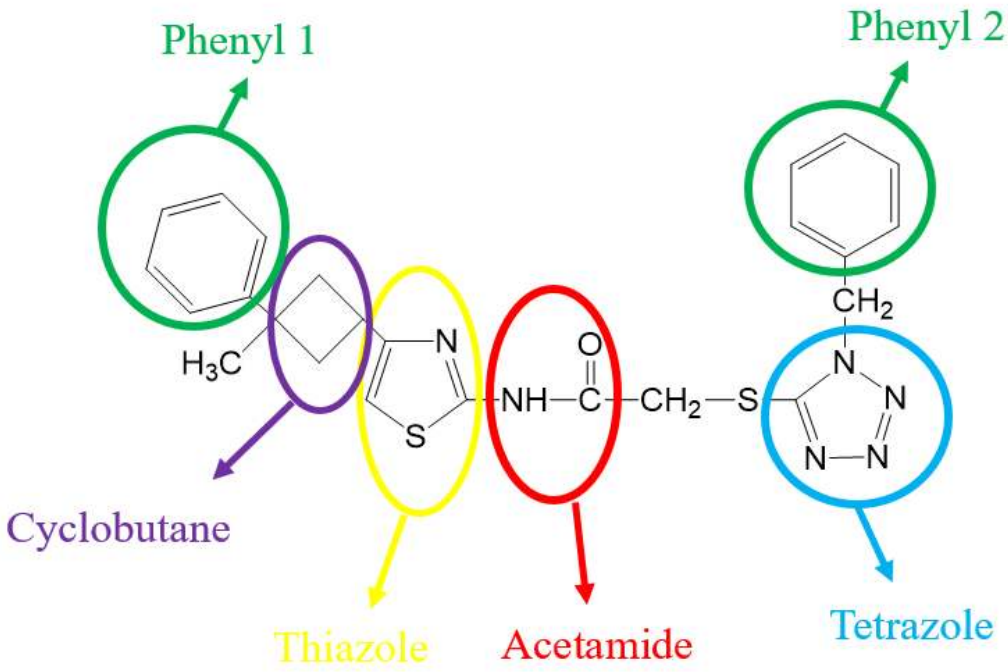

Figure 4.1 The chemical diagram of compound $C_{24}H_{24}N_6OS_2$ divided into chemical groups

The optimized molecular structures of the compound $C_{24}H_{24}N_6OS_2$ consisting of tetrazole, thiazole, cyclobutane, acetamide, and phenyl groups have been obtained in the ground state from water and ethanol solvents by DFT/B3LYP/6-311G and DFT/B3LYP/6-311G(d, p) methods.

The optimized molecular structures of the compound $C_{24}H_{24}N_6OS_2$ consisting of tetrazole, thiazole, cyclobutane, acetamide, and phenyl groups were obtained in the ground state from water and ethanol solvents by DFT/B3LYP/6-311G and DFT/B3LYP/6-311G(d, p) methods. Molecular structures corresponding to the lowest

energy, molecular orbital energy levels, and dipole moments of the molecular structure were obtained by single point energy calculations in ethanol and water by DFT/B3LYP/6-311G and DFT/B3LYP/6-311G(d, p) methods. The MEP map of the molecular structure was constructed using the DFT/B3LYP/6-311G(d, p) method in water. Similarly, Natural Population Analyses (NPA) charges of the molecular structure were found and Fukui functions were obtained using the DFT/B3LYP/6-311G(d, p) method in water. Using the molecular orbital energy values, the global reactivity parameters of the molecular structure were derived by DFT/B3LYP/6-311G and DFT/B3LYP/6-311G(d, p) methods for ethanol and water media, and the ΔN (charge transfer) and Electrophilicity-based Charge Transfer (ECT) parameters of the interaction with DNA bases such as Adenine (A), Guanine (G), Cytosine (C) and Thymine (T) were obtained.

4.1 The Optimization Study of the $C_{24}H_{24}N_6OS_2$

The geometric optimization of the $C_{24}H_{24}N_6OS_2$, which consists of different functional groups, was made by choosing the B3LYP/6-311G and B3LYP/6-311G(d, p) methods in water (ε=80.1, μ=1.82 D) and ethanol (ε=24.5, μ=1.69) environments with different dielectric constant and dipole moment. In Figure 4.2, it is given the optimized molecular structure of the $C_{24}H_{24}N_6OS_2$ by using B3LYP/6-311G(d, p) method in water media. The bond parameters obtained from the optimized molecular structures of the $C_{24}H_{24}N_6OS_2$ compound calculated by the B3LYP/6-311G method in water and ethanol environments are given in Table 4.1, and the bond parameters obtained by the B3LYP/6-311G(d, p) method are given in Table 4.2. The experimental bond parameters given in Table 4.1 and Table 4.2 are taken from the literature (Örnek 2019). The fit graphs of the experimental and theoretical bond parameters were drawn according to the regression analysis method. These fit graphs are given in Figure 4.3 and Figure 4.4. When the bond parameters of the $C_{24}H_{24}N_6OS_2$ calculated in water and ethanol environments were compared with both the experimental bond parameters in the literature and the theoretical values obtained from the gas environment, it was found that the bond parameter values obtained from the solvent environments were more compatible with the experimental values of the $C_{24}H_{24}N_6OS_2$.

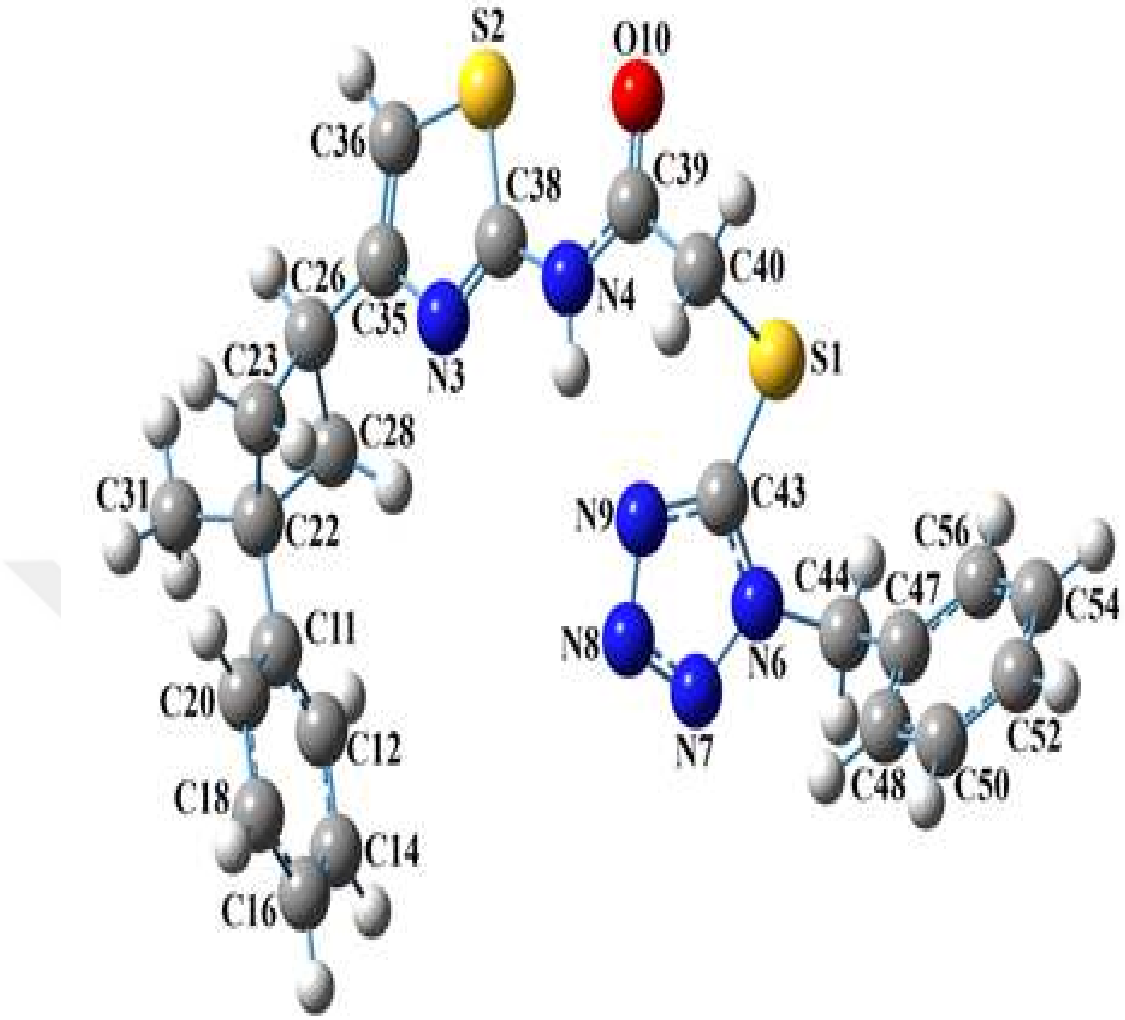

Figure 4.2 The optimized molecular structure of $C_{24}H_{24}N_6OS_2$ by using the B3LYP/6-311G(d, p) in the water media

According to the results of the regression analysis, the calculated both bond lengths and bond angles of the compound $C_{24}H_{24}N_6OS_2$ had the highest agreement with the experimental values. B3LYP/6-311G(d, p) ethanol> B3LYP/6-311G(d, p) water> B3LYP/6-311G ethanol> B3LYP/6-311G water can be given in the form. As can be seen from Table 4.1 and Table 4.2 and also from Figure 4.3 and Figure 4.4, the highest agreement in bond parameters was obtained from the ethanol medium. When compared with the values obtained from the gas environment in the literature (Örnek 2019), the bond parameters obtained from the solvent environment are more compatible with the experimental values compared to those obtained from the gas environment.

Table 4.1 The calculated bond parameters of $C_{24}H_{24}N_6OS_2$ by using the B3LYP/6-311G

$C_{24}H_{24}N_6OS_2$	**Experimental (Örnek 2019)**	**B3LYP/6-311G Water**	**B3LYP/6-311G Ethanol**
Bond lengths (Å)			
C52-C54	-	1.39715	1.39709
C54-C56	-	1.39885	1.39880
C56-C47	-	1.40075	1.40070
C48-C50	-	1.39610	1.39604
C50-C52	-	1.39985	1.39980
C47-C44	-	1.51724	1.51722
C44-N6	-	1.47361	1.47346
N6-N7	1.357(3)	1.38943	1.38990
N7-N8	1.288(3)	1.31535	1.31518
N8-N9	1.362(3)	1.39271	1.39298
N9-C43	1.314(3)	1.34070	1.34058
C43-N6	1.334(3)	1.35530	1.35525
C43-S1	1.738(2)	1.79720	1.79710
C40-C39	-	1.51074	1.51077
C39-O10	1.221(3)	1.25294	1.25279
C39-N4	1.340(3)	1.36933	1.36943
N4-C38	1.377(3)	1.38244	1.38267
C38-N3	1.300(3)	1.30531	1.30514
C38-S2	-	1.83361	1.83393
S2-C36	1.705(3)	1.81416	1.81394
S2-C38	1.721(2)	1.83361	1.83393
C36-C35	-	1.35973	1.35981
C35-N3	1.378(3)	1.40621	1.40604
C35-C26	-	1.49309	1.49303
C26-C28	-	1.56561	1.56557
C28-C22	-	1.57178	1.57178
C22-C11	-	1.51792	1.51784
C11-C20	-	1.40507	1.40493
C20-C18	-	1.39838	1.39829
C18-C16	-	1.39867	1.39857
C16-C14	-	1.39859	1.39850
C14-C12	-	1.39848	1.39836
C12-C11	-	1.40497	1.40486
R^2	-	0.99253	0.99254
Bond angles (°)			
C48-C50-C52	-	120.151	120.15187
C50-C52-C54	-	119.796	119.79779
C52-C54-C56	-	120.061	120.05853
C54-C56-C47	-	120.379	120.38077
C56-C47-C44	-	120.096	120.11808
C47-C44-N6	-	113.089	113.10158
N6-C43-S1	123.47(19)	125.26736	125.283
C44-N6-N7	121.0(2)	120.47405	120.46389
C44-N6-C43	131.4(2)	131.09580	131.120
N6-N7-N8	-	106.521	106.51837
N7-N8-N9	-	110.013	110.01877
N8-N9-C43	-	106.603	106.59432
N9-C43-S1	126.7(2)	126.28924	126.25394
C40-C39-N4	117.31(19)	115.78857	115.81073
C40-C39-O10	121.7(2)	121.09745	121.059

Table 4.1 The calculated bond parameters of $C_{24}H_{24}N_6OS_2$ by using the B3LYP/6-311G (Continued)

$C_{24}H_{24}N_6OS_2$	Experimental (Örnek 2019)	B3LYP/6-311G Water	B3LYP/6-311G Ethanol
Bond angles (°)			
O10-C39-N4	120.9(2)	123.09987	123.116
C39-N4-C38	125.00(18)	126.40120	126.342
N4-C38-S2	122.79(16)	123.61537	123.57252
N4-C38-N3	122.01(18)	121.95964	121.993
C38-S2-C36	-	86.023	86.00565
S2-C36-C35	-	111.680	111.69440
C35-C26-C28	-	118.275	118.34483
C26-C28-C22	-	89.389	89.36436
C28-C22-C11	-	117.054	117.07680
C22-C11-C12	-	120.877	120.86275
C11-C12-C14	-	120.960	120.96012
C12-C14-C16	-	120.191	120.18808
C14-C16-C18	-	119.452	119.45356
C16-C18-C20	-	120.193	120.19312
R^2	-	0.91571	0.91586
Torsion angles (°)			
C40-C39-N4-C38	176.1(2)	179.73084	179.63465
O10-C39-N4-C38	-2.03(3)	1.08542	0.992
C50-C48-C47-C44	-	178.233	178.25907
C47-C44-N6-N7	-60.8(3)	-102.77064	-102.502
C47-C44-N6-C43	118.8(3)	75.88060	76.088
C44-N6-N7-N8	179.1(3)	178.79190	178.75555
C44-N6-C43-N9	-179.2(3)	-178.95299	-178.919
C44-N6-C43-S1	0.6(4)	1.42349	1.438
N8-N9-C43-S1	-179.9(2)	-179.97552	-179.933
N7-N6-C43-S1	-	-179.802	-179.84311
S1-C43-N9-N8	-	-179.976	-179.93297
C39-N4-C38-N3	178.7(2)	178.81863	178.86398
C39-N4-C38-S2	-3.5(3)	-1.24574	-1.243
S2-C36-C35-C26	-	-179.829	-179.83505
C38-N3-C35-C26	-	179.824	179.84557
C35-C26-C23-C22	-	-138.342	-138.59806
C35-C26-C28-C22	-	138.404	138.64292
C23-C22-C11-C12	-	-142.001	-142.17076
C23-C22-C11-C20	-	40.362	40.20214
C22-C11-C12-C14	-	-177.874	-177.86185
C22-C11-C20-C18	-	177.879	177.86731
N4-C38-N3-C35	-	179.995	179.93252
C26-C28-C22-C11	-	-136.224	-136.42980
C26-C23-C22-C11	-	136.245	136.43723
C31-C22-C23-C26	-	-95.668	-95.46918
C43-S1-C40-C39	-	-85.224	-85.35460
C47-C44-N6-N7	-	-102.771	-102.50187
C47-C44-N6-C43	-	75.881	76.08801
C44-N6-C43-N9	-	-178.953	-178.91889
C44-N6-N7-N8	-	178.792	178.75555

Table 4.2 The calculated bond parameters of $C_{24}H_{24}N_6OS_2$ by using the B3LYP/6-311G(d, p)

$C_{24}H_{24}N_6OS_2$	Experimental (Örnek 2019)	B3LYP/6-311G(d, p) Water	B3LYP/6-311G (d, p) Ethanol
Bond lengths (Å)			
C52-C54	-	1.39284	1.39277
C54-C56	-	1.39492	1.39489
C56-C47	-	1.39619	1.39612
C48-C50	-	1.39194	1.39187
C50-C52	-	1.39568	1.39565
C47-C44	-	1.51575	1.51566
C44-N6	-	1.46933	1.46921
N6-N7	1.357(3)	1.35652	1.35684
N7-N8	1.288(3)	1.28335	1.28321
N8-N9	1.362(3)	1.35703	1.35720
N9-C43	1.314(3)	1.32511	1.32498
C43-N6	1.334(3)	1.34927	1.34923
C43-S1	1.738(2)	1.75204	1.75203
S1-C40	1.803(2)	1.84395	1.84397
C40-C39	-	1.52330	1.52337
C39-O10	1.221(3)	1.22188	1.22173
C39-N4	1.340(3)	1.36551	1.36556
N4-C38	1.377(3)	1.38533	1.38558
C38-N3	1.300(3)	1.30014	1.29996
C38-S2	-	1.75592	1.75607
S2-C36	1.705(3)	1.74365	1.74355
S2-C38	1.721(2)	1.75592	1.75607
C36-C35	-	1.36249	1.36255
C35-N3	1.378(3)	1.38389	1.38368
C35-C26	-	1.49523	1.49519
C26-C28	-	1.55844	1.55841
C28-C22	-	1.56320	1.56315
C22-C11	-	1.51631	1.51626
C11-C20	-	1.40029	1.40020
C20-C18	-	1.39440	1.39430
C18-C16	-	1.39427	1.39419
C16-C14	-	1.39445	1.39436
C14-C12	-	1.39415	1.39408
C12-C11	-	1.40053	1.40040
R^2	-	0.99788	0.99789
Bond angles (°)			
C48-C50-C52	-	120.16392	120.16301
C50-C52-C54	-	119.79480	119.79871
C52-C54-C56	-	120.04289	120.03996
C54-C56-C47	-	120.39120	120.39174
C56-C47-C44	-	119.97684	120.01036
C47-C44-N6	-	113.22534	113.23148
N6-C43-S1	123.47(19)	124.416	124.422
C44-N6-N7	121.0(2)	121.19084	121.19238
C44-N6-C43	131.4(2)	131.082	131.093
N6-N7-N8	-	107.05920	107.05589
N7-N8-N9	-	110.92262	110.92931
N8-N9-C43	-	106.13674	106.12902
C43-S1-C40	98.24(12)	100.13185	100.079

Table 4.2 The calculated bond parameters of $C24H_{24}N_6OS_2$ by using the B3LYP/6-311G(d, p) (Continued)

$C_{24}H_{24}N_6OS_2$	Experimental (Örnek 2019)	B3LYP/6-311G(d, p) Water	B3LYP/6-311G (d, p) Ethanol
Bond angles (°)			
N9-C43-S1	126.7(2)	127.40560	127.38226
S1-C40-C39	114.44574	114.44574	114.414
C40-C39-N4	117.31(19)	115.03533	115.04948
C40-C39-O10	121.7(2)	121.713	121.683
O10-C39-N4	120.9(2)	123.240	123.256
C39-N4-C38	125.00(18)	125.460	125.415
N4-C38-S2	122.79(16)	123.59735	123.57133
N4-C38-N3	122.01(18)	121.153	121.170
C38-S2-C36	-	87.73078	87.71550
S2-C36-C35	-	111.04992	111.05506
C35-C26-C28	-	118.33102	118.37823
C26-C28-C22	-	89.38726	89.36747
C28-C22-C11	-	117.04862	117.08515
C22-C11-C12	-	120.80716	120.81770
C11-C12-C14	-	121.02434	121.02180
C12-C14-C16	-	120.19308	120.19468
C14-C16-C18	-	119.39840	119.39895
C16-C18-C20	-	120.20846	120.20515
R^2	-	0.97844	0.97871
Torsion angles (°)			
C40-C39-N4-C38	176.1(2)	-179.56327	-179.56176
O10-C39-N4-C38	-2.03(3)	1.661	1.644
C50-C48-C47-C44	-	178.17009	178.22566
C47-C44-N6-N7	-60.8(3)	-101.807	-101.717
C47-C44-N6-C43	118.8(3)	76.107	76.186
C43-S1-C40-C39	-80.31(19)	-86.06831	-86.119
N6-C43-S1-C40	176.9(2)	-168.00413	-168.393
C44-N6-N7-N8	179.1(3)	178.38906	178.39748
C44-N6-C43-N9	-179.2(3)	-178.397	-178.409
C44-N6-C43-S1	0.6(4)	1.769	1.727
N8-N9-C43-S1	-179.9(2)	-179.790	-179.741
S1-C40-C39-O10	-62.7(3)	-101.32568	-101.096
S1-C40-C39-N4	119.24(19)	79.87817	80.089
N7-N6-C43-S1	-	179.89561	179.84418
S1-C43-N9-N8	-	-179.79018	-179.74087
C39-N4-C38-N3	178.7(2)	177.78103	177.82357
C39-N4-C38-S2	-3.5(3)	-2.756	-2.695
S2-C36-C35-C26	-	-179.48345	-179.48801
C38-N3-C35-C26	-	179.56461	179.56728
C35-C26-C23-C22	-	-138.57383	-138.77774
C35-C26-C28-C22	-	138.72322	138.92918
C23-C22-C11-C12	-	-143.17701	-143.03405
C23-C22-C11-C20	-	39.03625	39.18598
C22-C11-C12-C14	-	-178.06480	-178.04663
C22-C11-C20-C18	-	178.07521	178.05216
N4-C38-N3-C35	-	179.51691	179.53713
C26-C28-C22-C11	-	-136.58282	-136.73815
C26-C23-C22-C11	-	136.46561	136.64493
C31-C22-C23-C26	-	-95.55608	-95.39059

Table 4.2 The calculated bond parameters of $C_{24}H_{24}N_6OS_2$ by using the B3LYP/6-311G(d, p) (Continued)

$C_{24}H_{24}N_6OS_2$	Experimental (Örnek 2019)	B3LYP/6-311G(d, p) Water	B3LYP/6-311G (d, p) Ethanol
Torsion angles (°)			
C43-S1-C40-C39	-	-86.06831	-86.11899
C47-C44-N6-N7	-	-101.80712	-101.71655
C47-C44-N6-C43	-	76.10656	76.18630
C44-N6-C43-N9	-	-178.39652	-178.40938
C44-N6-N7-N8	-	178.38906	178.39748

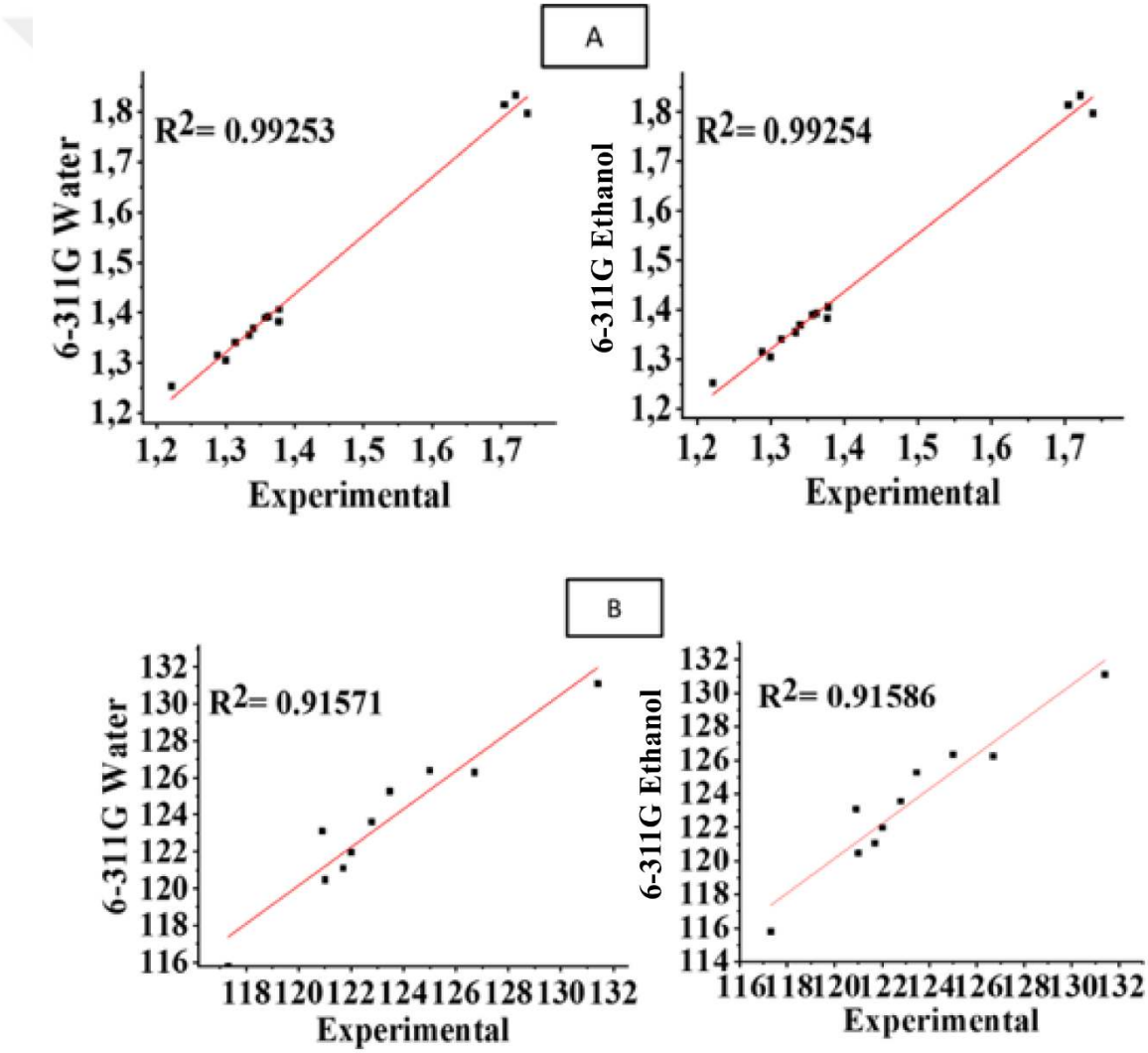

Figure 4.3 Compliance plots of the experimental and calculated by using the B3LYP/6-311G A) bond lengths B) bond angles of the $C_{24}H_{24}N_6OS_2$

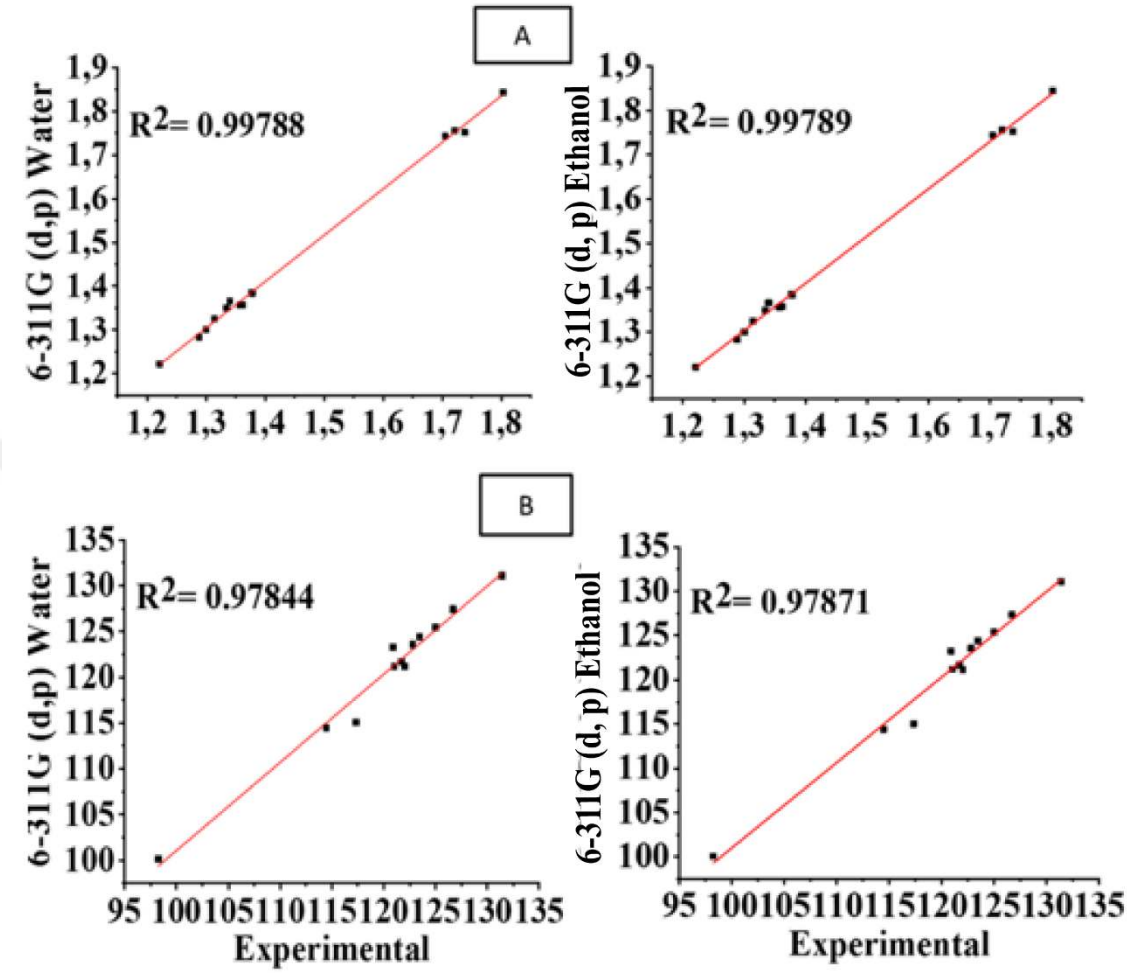

Figure 4.4 Compliance plots of the experimental and calculated by using the B3LYP/6-311G(d, p) A) bond lengths B) bond angles of the $C_{24}H_{24}N_6OS_2$

4.2 The Energy Study of the $C_{24}H_{24}N_6OS_2$

Using the optimized molecular structure of $C_{24}H_{24}N_6OS_2$, the total energy, dipole moment, the molecular orbital energy values of the $C_{24}H_{24}N_6OS_2$ were calculated in both water and ethanol environments by choosing the B3LYP/6-311G and 6-311G(d, p) methods. One of the parameters that determine the stability of a molecular structure is the total energy of the $C_{24}H_{24}N_6OS_2$. The structure with the lowest total energy constitutes the most stable structure (Table 4.3).

Table 4.3 The calculated molecular orbital energy values, the total energies and HOMO-LUMO energy gaps (ΔE) of $C_{24}H_{24}N_6OS_2$ by the DFT method

$C_{24}H_{24}N_6OS_2$	E_{HOMO} (eV)	E_{LUMO} (eV)	Total energy (a.u)	μ (D)	ΔE (eV)
B3LYP/6-311G Water	-6.4684	-1.9129	-2128.9788	6.6585	4.5555
B3LYP/6-311G Ethanol	-6.4521	-1.9039	-2128.9774	6.6280	4.5482
B3LYP/6-311G(d, p) Water	-6.2559	-1.4340	-2129.4658	6.2786	4.8219
B3LYP/6-311G(d, p) Ethanol	-6.2417	-1.4258	-2129.4646	6.2418	4.8159

Another stability parameter is the difference between the molecular orbital energy levels of the molecular structure. Electrons fill molecular orbital energy levels starting from the lowest energy. The energy level of a molecular structure that acts as a donor is the highest molecular orbital (HOMO), and the energy level that acts as an acceptor is the lowest molecular orbital (LUMO). The narrower this energy level ΔE, the softer and chemically active the molecule, the wider the molecule, the harder and chemically reactive it is.

To understand in which solvent environment the molecular structure $C_{24}H_{24}N_6OS_2$ is more stable, single-point energy calculations were made in the ground state and the results are given in Table 4.3. As can be seen from Table 4.3, it was found that the medium with the lowest total energy was obtained from the water environment by the B3LYP/6-311G(d, p) method with a total energy value of -2129.4658 a.u. Likewise, the widest ΔE (4.8219 eV) range was obtained from the water environment by the B3LYP/6-311G(d, p) method and it was found that the structure was harder and chemically reactive in this environment compared to the others.

The MEP surface of the $C_{24}H_{24}N_6OS_2$ was obtained from the water environment by performing a single-point energy calculation with the B3LYP/6-311G(d, p) method in the ground state. MEP surfaces define electron-rich and poor regions in a molecule. It allows for predicting from which region the molecular structures can bond with another molecular structure. In Figure 4.5, the MEP surface of the $C_{24}H_{24}N_6OS_2$ is given.

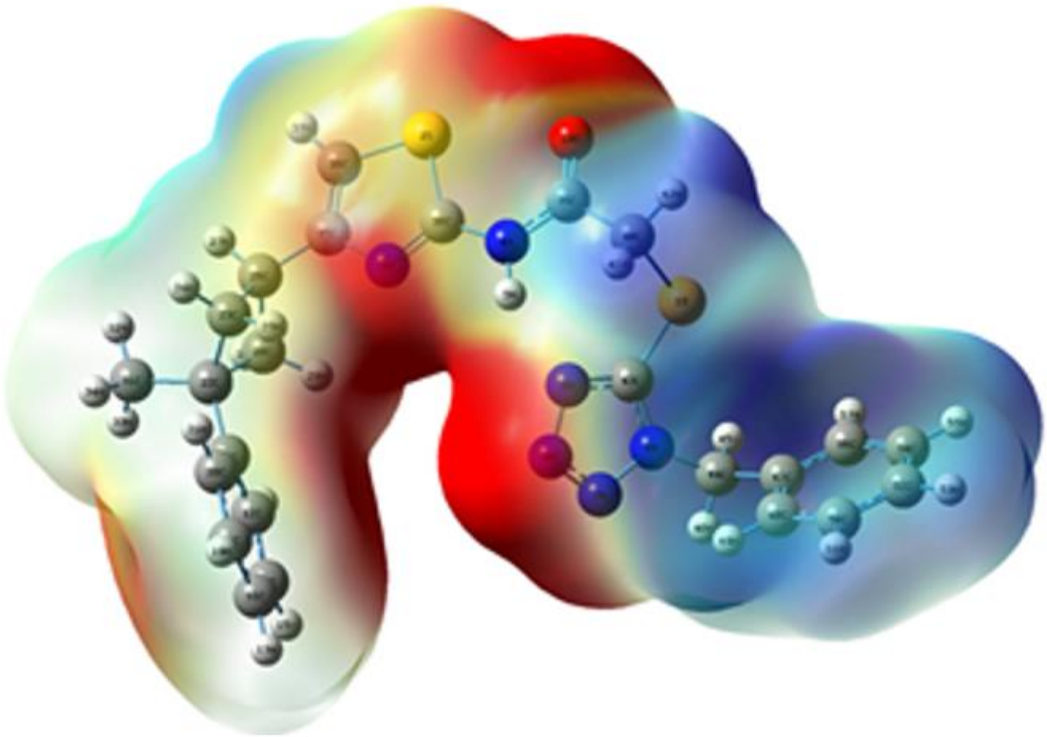

Figure 4.5 The calculated MEP surface of the $C_{24}H_{24}N_6OS_2$ by using the B3LYP/6-311G(d, p) in water media

As seen in Figure 4.5, the electron-rich region (red color=nucleophilic region) is tetrazole, thiazole, acetamide, and phenyl 1 group, while the electron-poor region (blue color=electrophilic) is phenyl 2 group and CH_2 groups.

4.3 The Fukui Functions of the $C_{24}H_{24}N_6OS_2$

In this thesis, the Fukui functions of the $C_{24}H_{24}N_6OS_2$ have been obtained from the Natural Population Analysis (NPA) charges by the energy calculations in the water environment with the B3LYP/6-311G(d, p) method. Fukui functions help us identify reactive atoms in a molecule. The reactivity of a molecule is very important for the molecules planned to be synthesized and for the biological activities of the molecules. Table 4.4, it is given the calculated NPA charges of the $C_{24}H_{24}N_6OS_2$ by the B3LYP/6-311G(d, p) method in water media. The Fukui functions derived from the NPA charges of the $C_{24}H_{24}N_6OS_2$ are given in Table 4.5.

Table 4.4 The calculated NPA charges of the $C_{24}H_{24}N_6OS_2$ by using the B3LYP/6-311G(d, p) method in water media

B3LYP/6-311G (d, p)				B3LYP/6-311G (d, p)			
Atoms	q_k(N)	q_k $(N+1)$	q_k $(N-1)$	**Atoms**	q_k(N)	q_k $(N+1)$	q_k $(N-1)$
S1	0.30629	0.32828	0.15252	H30	0.19905	0.21486	0.19478
S2	0.38349	0.52797	0.27823	C31	-0.56376	-0.56614	-0.56313
N3	-0.54473	-0.49875	-0.61820	H32	0.19726	0.19861	0.19692
N4	-0.63244	-0.56054	-0.63587	H33	0.19937	0.20457	0.19781
H5	0.45177	0.47078	0.43680	H34	0.19937	0.20467	0.19780
N6	-0.21382	-0.21141	-0.22287	C35	0.14704	0.29181	0.13852
N7	-0.07499	-0.06881	-0.09547	C36	-0.41419	-0.20737	-0.48331
N8	-0.06947	-0.06451	-0.08554	H37	0.23789	0.26759	0.22126
N9	-0.42020	-0.42634	-0.42908	C38	0.27539	0.36875	0.22638
O10	-0.63432	-0.56769	-0.74851	C39	0.69224	0.70745	0.54903
C11	-0.02629	-0.03235	-0.02449	C40	-0.55795	-0.56489	-0.59841
C12	-0.21333	-0.21142	-0.21374	H41	0.24727	0.25622	0.22045
H13	0.20824	0.20913	0.20798	H42	0.25345	0.26380	0.22573
C14	-0.19769	-0.19529	-0.19831	C43	0.23508	0.23570	0.22713
H15	0.20681	0.20853	0.20630	C44	-0.19096	-0.19135	-0.19215
C16	-0.21779	-0.21357	-0.21900	H45	0.22734	0.22822	0.22118
H17	0.20704	0.20855	0.20657	H46	0.24086	0.24208	0.22935
C18	-0.19761	-0.19491	-0.19825	C47	-0.05555	-0.05684	-0.05161
H19	0.20679	0.20851	0.20627	C48	-0.20182	-0.20151	-0.21428
C20	-0.21354	-0.21185	-0.21399	H49	0.21448	0.21458	0.21220
H21	0.20836	0.20927	0.20809	C50	-0.19177	-0.19157	-0.19477
C22	-0.03769	-0.03378	-0.03920	H51	0.21248	0.21282	0.20979
C23	-0.36558	-0.34447	-0.36799	C52	-0.19783	-0.19608	-0.20667
H24	0.19902	0.21474	0.19475	H53	0.21185	0.21191	0.20919
H25	0.20579	0.21539	0.20426	C54	-0.19437	-0.19428	-0.20399
C26	-0.22697	-0.25333	-0.22193	H55	0.21287	0.21323	0.20999
H27	0.21227	0.23241	0.20528	C56	-0.19858	-0.19826	-0.20087
C28	-0.36450	-0.34191	-0.36687	H57	0.21366	0.21389	0.21062
H29	0.20493	0.21491	0.20334				

While the MEP surface of a molecular structure describes the nucleophilic-electrophilic regions, the Fukui functions enable the identification of nucleophilic-electrophilic atoms in a molecular structure (Pucci and Angilella 2022).

k Fukui functions of atoms are given in Equation (4.1), Equation (4.2) and Equation (4.3)

$$f_k^- = q_k(N) - q_k(N-1) \tag{4.1}$$

$$f_k^+ = q_k(N+1) - q_k(N) \tag{4.2}$$

$$f_k^0 = \frac{1}{2}[q_k(N+1) - q_k(N-1)] \quad (4.3)$$

In these equations, q_k is in neutral (N), anionic (N+1) or cationic (N-1) chemical species representing the atomic region of the atom k. The positive values of $f_k^-(r)$, $f_k^+(r)$, and $f_k^0(r)$ give electrophilic, nucleophilic, and radical atoms in the molecular structure, respectively (Fukui 2006, Parr *et al.* 1978) (Table 4.5).

Table 4.5 Fukui functions obtained from NPA charges of the $C_{24}H_{24}N_6OS_2$ by using the B3LYP/6-311G(d, p) method in water media

B3LYP/6-311G (d, p)				B3LYP/6-311G (d, p)			
Atoms	fk^0	fk^+	fk^-	**Atoms**	fk^0	fk^+	fk^-
S1	0.08788	0.02199	0.15377	H30	0.01004	0.01581	0.00427
S2	0.12487	0.14448	0.10526	C31	-0.00150	-0.00238	-0.00063
N3	0.059725	0.04598	0.07347	H32	0.000845	0.00135	0.00034
N4	0.037665	0.0719	0.00343	H33	0.00338	0.0052	0.00156
H5	0.01699	0.01901	0.01497	H34	0.003435	0.0053	0.00157
N6	0.00573	0.00241	0.00905	C35	0.076645	0.14477	0.00852
N7	0.01333	0.00618	0.02048	C36	0.13797	0.20682	0.06912
N8	0.010515	0.00496	0.01607	H37	0.023165	0.0297	0.01663
N9	0.00137	-0.00614	0.00888	C38	0.071185	0.09336	0.04901
O10	0.09041	0.06663	0.11419	C39	0.07921	0.01521	0.14321
C11	-0.00393	-0.00606	-0.0018	C40	0.01676	-0.00694	0.04046
C12	0.00116	0.00191	0.00041	H41	0.017885	0.00895	0.02682
H13	0.000575	0.00089	0.00026	H42	0.019035	0.01035	0.02772
C14	0.00151	0.0024	0.00062	C43	0.004285	0.00062	0.00795
H15	0.001115	0.00172	0.00051	C44	0.0004	-0.00039	0.00119
C16	0.002715	0.00422	0.00121	H45	0.00352	0.00088	0.00616
H17	0.00099	0.00151	0.00047	H46	0.006365	0.00122	0.01151
C18	0.00167	0.0027	0.00064	C47	-0.00261	-0.00129	-0.00394
H19	0.00112	0.00172	0.00052	C48	0.006385	0.00031	0.01246
C20	0.00107	0.00169	0.00045	H49	0.00119	0.0001	0.00228
H21	0.00059	0.00091	0.00027	C50	0.0016	0.0002	0.003
C22	0.00271	0.00391	0.00151	H51	0.001515	0.00034	0.00269
C23	0.01176	0.02111	0.00241	C52	0.005295	0.00175	0.00884
H24	0.009995	0.01572	0.00427	H53	0.00136	0.00006	0.00266
H25	0.005565	0.0096	0.00153	C54	0.004855	0.0001	0.00962
C26	-0.0157	-0.02636	-0.00504	H55	0.00162	0.00036	0.00288
H27	0.013565	0.02014	0.00699	C56	0.001305	0.00032	0.00229
C28	0.01248	0.02259	0.00237	H57	0.001635	0.00023	0.00304
H29	0.005785	0.00998	0.00159				

According to the calculation results, the most nucleophilic atoms of the $C_{24}H_{24}N_6OS_2$ are C(36)>C(35)>S(2)>O(10) and the most electrophilic atoms are S(1)>C(39)>O(10)>S(2) form was found.

4.4 Interaction Study of the $C_{24}H_{24}N_6OS_2$ with DNA Bases

The $C_{24}H_{24}N_6OS_2$ molecular structure was optimized in the water and ethanol environments by choosing the B3LYP/6-311G and B3LYP/6-311G(d, p) methods, and a single point energy calculations were made in the ground state. By using the molecular orbital energy values (HOMO and LUMO values) obtained from the calculation results, global reactivity parameters can be derived from the chemical and physical parameters of the molecular structure. Reactivity parameters are needed to investigate the interaction of the $C_{24}H_{24}N_6OS_2$ molecular structure with DNA bases such as adenine, guanine, cytosine, and thymine. When a molecular structure is used as a drug substance, it will react with DNA bases in the water environment. Considering this situation, the calculation results are taken from the water environment.

To remove an electron from a molecule, the ionization potential (IP) is where the energy is lowest. The energy that a molecule gains when it receives an additional electron is referred to as "electron affinity" (EA). An atom's capacity to draw shared electrons to itself is determined by its electronegativity (χ). The tendency of an electron to leave a system in equilibrium is represented by the chemical potential (μ_X). The electronegativity is the inverse of it. Measured by a molecule's resistance to intramolecular charge transfer, chemical hardness (η) is a unit of analysis. The electrophilicity index (ω), which is calculated by dividing the chemical potential by its square, by its chemical hardness, serves as a measure of the stabilizing energy when a system acquires an extra electronic charge from the environment. Chemical hardness (η) and global softness (S) are negatively related (Pearson 1997).

These parameters of the $C_{24}H_{24}N_6OS_2$ are defined as Equation (4.4), Equation (4.5), Equation (4.6), Equation (4.7), Equation (4.8), Equation (4.9), and Equation (4.10);

$$IP = -E_{HOMO} \tag{4.4}$$

$$EA = -E_{LUMO} \tag{4.5}$$

$$\chi = \frac{(IP+EA)}{2} \quad (4.6)$$

$$\mu = -\chi \quad (4.7)$$

$$\eta = \frac{(IP-EA)}{2} \quad (4.8)$$

$$\omega = \frac{\mu^2}{2\eta} \quad (4.9)$$

$$S = \frac{1}{2\eta} \quad (4.10)$$

The ECT (electrophilicity-based charge transfer) approach and ΔN (charge transfer) parameters are derived from the obtained reactivity parameters. The ΔN parameter consists of chemical potential and chemical hardness, and the ECT parameter consists of electronegativity and electrophilicity index.

If we consider two interacting systems, A and B, we can write the ΔN parameter as the Equation (4.11), with μ_A and μ_B being the chemical potentials of these systems and η_A and η_B being their chemical hardness.

$$\Delta N = \frac{\mu_B-\mu_A}{2(\eta_A+\eta_B)} \quad (4.11)$$

Another approximation used to determine the magnitude and direction of charge transfer in two interacting systems (A and B) is the ECT approximation. This approximation is given in Equation (4.12).

$$ECT = (\Delta N_{max})_A - (\Delta N_{max})_B = 2[\omega_A X_A - \omega_B X_B] \quad (4.12)$$

X in Equation 4.12 represents the opposite of electronegativity (1/χ) and ω represents electronegativity. If the ECT value is negative, system A acts as a donor, and the charge

flow is A$\xrightarrow{charge\ transfer}$B. If it is positive, system B acts as an acceptor the opposite flow is B $\xrightarrow{charge\ transfer}$ A.

The global reactivity parameters of $C_{24}H_{24}N_6OS_2$ were derived using the HOMO and LUMO energy values in Table 4.3 and given in Table 4.6 by using DFT/B3LYP/6-311G and DFT/B3LYP/6-311G(d, p) in water and ethanol media.

Table 4.6 The global reactivity parameters of the $C_{24}H_{24}N_6OS_2$

$C_{24}H_{24}N_6OS_2$	B3LYP/6-311G Water	B3LYP/6-311G Ethanol	B3LYP/6-311G(d, p) Water	B3LYP/6-311G(d, p) Ethanol
IP (eV)	6.4684	6.4521	6.2559	6.2417
EA (eV)	1.9129	1.9039	1.4340	1.4258
μ_x (eV)	-4.1906	-4.178	-3.8449	-3.8337
χ (eV)	4.1906	4.178	3.8449	3.8337
η (eV)	2.2777	2.2741	2.4109	2.4079
S (eV^{-1})	0.2195	0.2198	0.2073	0.2076
ω (eV)	3.8550	3.8379	3.0659	3.0518

The lower the electrophilicity index value of a molecule, the more nucleophilic the molecule is; that is, because it is rich in electrons, it is prone to donate electrons and can act as a donor. As seen in Table 4.6, the lowest electrophilicity index (ω) value was obtained with the B3LYP/6-311G(d, p) method. The result obtained from both solvent media is close to each other. The chemical hardness (η) value of the $C_{24}H_{24}N_6OS_2$ with the highest value was found in the water environment by the B3LYP/6-311G(d, p) method.

Table 4.7 and Table 4.8 contain the ECT and ΔE parameters obtained to explain the interaction of the molecular structure with the DNA bases. As seen in both tables, the highest interaction of $C_{24}H_{24}N_6OS_2$ the molecular structure was with G base from DNA bases. The negative values in the parameters show that the charge transfer is from the G base to the Molecular structure (G base$\xrightarrow{charge\ transfer}$ the $C_{24}H_{24}N_6OS_2$). As can be seen from the electrophilicity index values, the lowest value was found in the G base, and it was found that the DNA bases showed a more nucleophilic effect than the $C_{24}H_{24}N_6OS_2$.

Table 4.7 ΔN and ECT parameters (B: $C_{24}H_{24}N_6OS_2$, A: DNA bases) obtained by using DFT/B3LYP/6-311G in water media

	A Base	G Base	C Base	T Base	$C_{24}H_{24}N_6OS_2$
Total Energy (a.u.)	-467.2879	-542.5358	-394.9330	-453.4397	-2128.9788
IP (eV)	6.40806	6.06928	6.65215	6.96209	6.4684
EA (eV)	1.05391	0.76383	1.20058	1.47351	1.9129
μx (eV)	-3.73099	-3.41656	-3.92637	-4.21780	-4.1906
χ (eV)	3.73099	3.41656	3.92637	4.21780	4.1906
η (eV)	2.67708	2.65273	2.72579	2.74470	2.2777
S (eV^{-1})	0.13953	0.14211	0.13459	0.13274	0.2195
ω (eV)	2.59990	2.20016	2.82787	3.24076	3.8550
ΔN	-0.04637	-0.15105	-0.02640	0.00271	
ECT	-0.44616	-0.55190	-0.39938	-0.30314	

Table 4.8 ΔN and ECT parameters (B: $C_{24}H_{24}N_6OS_2$, A: DNA bases) obtained by using DFT/B3LYP/6-311G(d, p) in water media

	A Base	G Base	C Base	T Base	$C_{24}H_{24}N_6OS_2$
Total Energy (a.u.)	-467.4530	-542.7224	-395.0623	-453.5874	-2129.4658
IP (eV)	6.23935	5.87254	6.55146	6.81923	6.2559
EA (eV)	0.80900	0.42042	0.99785	1.13255	1.4340
μx (eV)	-3.52418	-3.14648	-3.77466	-3.97589	-3.8449
χ (eV)	3.52418	3.14648	3.77466	3.97589	3.8449
η (eV)	2.71518	2.72606	2.77680	2.84334	2.4109
S (eV^{-1})	0.18415	0.18341	0.18006	0.17585	0.2073
ω (eV)	2.28711	1.81587	2.56555	2.77978	3.0659
ΔN	-0.03128	-0.06798	-0.00677	0.01247	
ECT	-0.60534	-0.74908	-0.54394	-0.50498	

5. CONCLUSIONS AND RECOMMENDATION

5.1 Conclusions

- When the bond parameters of the $C_{24}H_{24}N_6OS_2$ optimized molecular structure are examined, it can be said that these parameters are more compatible with the B3LYP/6-311G(d, p) method and ethanol media when the bond parameters are compared with the experimental values in the literature.
- Single point energy calculation results of the $C_{24}H_{24}N_6OS_2$ optimized molecular structure show that the $C_{24}H_{24}N_6OS_2$ molecular structure reaches the lowest energy, that is, the most stable state, in the water environment with the B3LYP/6-311G(d, p) method.
- The single point energy calculation of the $C_{24}H_{24}N_6OS_2$ molecular structure results show that the ΔE energy range of the molecular structure is wider with the B3LYP/6-311G(d, p) method and in the water environment, that is, the structure is more rigid and chemically reactive in this environment.
- The obtained MEP surface of $C_{24}H_{24}N_6OS_2$ the molecular structure shows that the tetrazol, thiazole, acetamide, and phenyl 1 groups are more nucleophilic, while the phenyl 2 and CH_2 groups are more electrophilic.
- The calculated Fukui function results of $C_{24}H_{24}N_6OS_2$ the molecular structure show that the atoms with the highest nucleophilic value of the molecular structure are in the atoms of the thiazole and acetamide groups, and the atoms with the highest electrophilic value are in the S1 atom and the acetamide C39 atom.
- The electrophilicity index value of $C_{24}H_{24}N_6OS_2$ the molecular structure was found to be the lowest among the global reactivity parameters, using the B3LYP/6-311G(d, p) method. Although the values obtained from both water and ethanol solvent media are close to each other, the lowest electrophilicity index value was obtained from the ethanol medium. The molecular structure has a more nucleophilic effect in this environment than in the water environment.
- The highest chemical hardness value of $C_{24}H_{24}N_6OS_2$ the molecular structure was found in the water environment with the B3LYP/6-311G(d, p) method. The fact that the HOMO-LUMO interval is wide in this environment also supports the results.

- In the interaction of $C_{24}H_{24}N_6OS_2$ the molecular structure with the DNA bases, both the calculated ΔE and ECT parameters show that $C_{24}H_{24}N_6OS_2$ the molecular structure has the highest interaction with the Guanine base, one of the DNA bases. In this interaction, it can be said that the DNA bases are more nucleophilic than the molecular structure and the charge transfer will be from the DNA bases to the molecular structure (Guanine base $\xrightarrow{charge\ transfer}$ $C_{24}H_{24}N_6OS_2$ the molecular structure) $C_{24}H_{24}N_6OS_2$ the molecular structure). According to the values obtained from both the MEP results and the Fukui functions of $C_{24}H_{24}N_6OS_2$ the molecular structure, it can be said that the interaction between DNA bases and the molecular structure will be mostly through the phenyl 2, CH_2 group, sulfur atom, and the acetamide oxygen atom of the molecular structure.

5.2 Recommendations

- Using the most stable molecular structure of $C_{24}H_{24}N_6OS_2$ the molecular structure obtained from this thesis study, its interaction with protein structures can be investigated by molecular docking study.
- The physical and chemical properties of $C_{24}H_{24}N_6OS_2$ the molecular structure from different solvent environments can be investigated and compared.

REFERENCES

Al-Saadi, M. S., Faidallah, H. M. and Rostom, S. A. 2008. Synthesis and biological evaluation of some 2, 4, 5-trisubstituted thiazole derivatives as potential antimicrobial and anticancer agents. Archiv der Pharmazie: An International Journal Pharmaceutical and Medicinal Chemistry, 341(7): 424-434.

Andreoni, W. and Curioni, A. 2002. Towards the design of functional materials and drugs 'from Scratch'. Ercim News, 2(1).

Becke, A. D. 1993. Density-functional thermochemistry. III. The role of exact exchange. The Journal of Chemical Physics, 98(7): 5648-6.

Benson, F. R. 1947. The chemistry of the tetrazoles. Chemical Reviews, 41(1): 1-61.

Bhatt, U. 2011. Five-membered heterocycles with four heteroatoms: tetrazoles. Modern Heterocyclic Chemistry, 1401-1430.

Bladin, J. A. 1885. Ueber von dicyanphenylhydrazin abgeleitete verbindungen. Berichte der Deutschen Chemischen Gesellschaft, 18(1): 1544-1551.

Booth, M. J., Raiber, E. A. and Balasubramanian, S. 2015. Chemical methods for decoding cytosine modifications in DNA. Chemical Reviews, 115(6): 2240-2254.

Bransden B. H. and Joachain, C. J. 2003. Physics of atoms and molecules. Pearson Education, 1114 page, Londra.

Cai, W. X., Liu, A. L., Li, Z. M., Dong, W. L., Liu, X. H. and Sun, N. B. 2016. Synthesis and anticancer activity of novel thiazole-5-carboxamide derivatives. Applied Sciences, 6(1): 8.

Camargo, A. J., Honório, K. M., Mercadante, R., Molfetta, F. A., Alves, C. N. and Da Silva, A. B. 2003. A study of neolignan compounds with biological activity against Paracoccidioides brasiliensis by using quantum chemical and chemometric methods. Journal of the Brazilian Chemical Society, 14: 809-814.

Carell, T., Kurz, M. Q., Müller, M., Rossa, M. and Spada, F. 2018. Non-canonical bases in the genome: the regulatory information layer in DNA. Angewandte Chemie International Edition, 57(16): 4296-4312.

Chauhan, R., Saini, P., Choudhary, R. and Rani, S. 2020. A review on pharmacological profile of Ethanamide and their derivatives. International Journal of Pharmaceutical Sciences Review and Research, 64: 162-170.

Cramer, C. J. 2013. Essentials of computational chemistry: Theories and models. John Wiley & Sons, 624 page, New York.

Devine, K. G. and Jheeta, S. 2020. De novo nucleic acids: a review of synthetic alternatives to DNA and RNA that could act as bio-information storage molecules. Life, 10(12): 346.

Dorsett, H. and White, A. 2000. Overview of molecular modelling and ab initio molecular orbital methods suitable for use with energetic materials. Defence Science and Technology Organization 9(1).

El-Sayed, W. A., Abdel-Monem, Y. K., Yousif, N. M., Tawfek, N., Shaaban, M. T. and Abdel-Rahman, A. A. H. 2009. Antimicrobial activity of new 2, 4-disubstituted thiazolidinone derivatives. Zeitschrift für Naturforschung C, 64(11-12): 785-789.

Eschrig, H. 1996. The fundamentals of density functional theory. Stuttgart Teubner, 204 page, Stuttgart.

Fermi, E. 1927. Statistical method to determine some properties of atoms. Accademia Nazionale dei Lincei, 6(602): 5.

Fitts, D. D. 1999. Principles of quantum mechanics: as applied to chemistry and chemical physics. Cambridge University Press, 351 page, Cambridge.

Floros, M. C., Bortolatto, J. F., Oliveira Jr, O. B., Salvador, S. L. and Narine, S. S. 2016. Antimicrobial activity of amphiphilic triazole-linked polymers derived from renewable sources. ACS Biomaterials Science & Engineering, 2(3): 336-343.

Frisch, M. J., Trucks, G. W., Schlegel, H. B., Scuseria, G. E., Robb, M. A., Cheeseman, J. R. and Fox, D. J. 2009. Gaussian 09 revision A. Gaussian Incorporated, 139.

Fukui, K. 2006. Theory of orientation and stereoselection. In Orientation and Stereoselection. Berlin, Heidelberg: Springer Berlin Heidelberg, 1-85.

Gotwals, R. R. and Sendlinger, S. C. 2007. A chemistry educator's guide to molecular modeling. ResearchGate, 17(1).

Gupta, R., Fuloria, N. K. and Fuloria, S. 2013. Synthesis and antimicrobial activity evaluation of some schiff bases derived from 2-aminothiazole derivatives. Indonesian Journal of Pharmacy, 193-197.

Gupta, V. and Kant, V. 2013. A review on biological activity of imidazole and thiazole moieties and their derivatives. Science International, 1(7): 253-260.

Hassan, F. A. 2012. Synthesis, characterization, anti-inflammatory, and antioxidant activities of some new thiazole derivatives. International Journal of Applied Science and Technology, 2(7): 180-187.

Horton, D. A., Bourne, G. T. and Smythe, M. L. 2003. The combinatorial synthesis of bicyclic privileged structures or privileged substructures. Chemical Reviews, 103(3): 893-930.

Jensen, F. 2017. Introduction to computational chemistry. John Wiley & Sons, 664 page, New York.

Kampen, H. M., Méndez, H. and Zahn, D. R. T. 1999. Energy level alignment at molecular semiconductor/GaAs (100) Interaces: where is the LUMO. University of Chemnitz, Institut für Physik, 1-8.

Kasai, S., Nagasawa, H., Yamashita, M., Masui, M., Kuwasaka, H., Oshodani, T. and Hori, H. 2001. New antimetastatic hypoxic cell radiosensitizers: design, synthesis, and biological activities of 2-nitroimidazole-acetamide, TX-1877, and its analogues. Bioorganic & Medicinal Chemistry, 9(2): 453-464.

Khan, K. M., Qurban, S., Salar, U., Taha, M., Hussain, S., Perveen, S. and Wadood, A. 2016. Synthesis, in vitro α-glucosidase inhibitory activity and molecular docking studies of new thiazole derivatives. Bioorganic Chemistry, 68: 245-258.

Kohanoff, J. and Gidopoulos, N. I. 2003. Density functional theory: basics, new trends and applications. Handbook of Molecular Physics and Quantum Chemistry, 2(5): 532-568.

Kwon, O., Coropceanu, V., Gruhn, N. E., Durivage, J. C., Laquindanum, J. G., Katz, H. E. and Brédas, J. L. 2004. Characterization of the molecular parameters determining charge transport in anthradithiophene. The Journal of Chemical Physics, 120(17): 8186-8194.

Lazarević, T., Rilak, A. and Bugarčić, Ž. D. 2017. Platinum, palladium, gold and ruthenium complexes as anticancer agents: Current clinical uses, cytotoxicity studies and future perspectives. European Journal of Medicinal Chemistry, 142: 8-31.

Lee, C., Yang, W. and Parr, R. G. 1988. Development of the Colle-Salvetti correlation-energy formula into a functional of the electron density. Physical Review B, 37(2): 785.

Lipkowitz, K. B. and Boyd, D. B. 2008. Reviews in computational chemistry. John Wiley & Sons, 568 page, New York.

Luo, C., Hajkova, P. and Ecker, J. R. 2018. Dynamic DNA methylation: In the right place at the right time. Science, 361(6409): 1336-1340.

Minkin, V. I. 1999. Glossary of terms used in theoretical organic chemistry. Pure and Applied Chemistry, 71(10): 1919-1981.

Mueller M. P. 2007. Fundamentals of quantum chemistry: Molecular spectroscopy and modern electronic structure computations. Springer Science & Business Media, 265 page, Berlin.

Nalawade, A. M., Nalawade, R. A., Patange, S. M. and Tase, D. R. 2013. Thiazole Containing Schiff bases and their transition metal complexes. The International Journal of Engineering Science, 2(7): 1-4.

Neochoritis, C. G., Zhao, T. and Dömling, A. 2019. Tetrazoles via multicomponent reactions. Chemical Reviews, 119(3): 1970-2042.

Örnek, M. 2019. Tetrazol, Tiyazol, Triazin ve Siklobütil içeren tek kristal yapıların deneysel ve hesaplamalı kimya yöntemleriyle aydınlatılması. MSc. Thesis, Çankırı Karatekin Üniversitesi, 101 page, Çankırı.

Parr, R. G., Donnelly, R. A., Levy, M. and Palke, W. E. 1978. Electronegativity: the density functional viewpoint. The Journal of Chemical Physics, 68(8): 3801-3807.

Pearson, R. G. 1997. Chemical hardness. Weinheim, 10: 3527606173.

Pucci, R. and Angilella, G. G. N. 2006. Majorana: from atomic and molecular, to nuclear physics. Foundations of Physics, 36: 1554-1572.

Pucci, R. and March, N. H. 1982. Total energy of atomic ions related to low-order ionization potentials and to diamagnetic susceptibility. The Journal of Chemical Physics, 76(12): 6091-6094.

Pucci, R. and Angilella, G. G. N. 2022. Density functional theory, chemical reactivity, and the Fukui functions. Foundations of Chemistry, 24(1): 59-71.

Raiber, E. A., Hardisty, R., Van Delft, P. and Balasubramanian, S. 2017. Mapping and elucidating the function of modified bases in DNA. Nature Reviews Chemistry, 1(9): 0069.

Rajasekaran, A. and Murugesan, S. 2005. Synthesis and characterization of some novel azetidinone derivatives as anti-bacterial and anti-convulsant agents. Journal of Pharmacy & Bioresources, 2(2): 162-168.

Ramsay, J. O. and Silverman, B. W. 2005. From functional data to smooth functions. Functional Data Analysis, 37-58.

Reimers, J. R. 2011. Computational methods for large systems: electronic structure approaches for biotechnology and nanotechnology. John Wiley & Sons, 688 page, New York.

Ripain, I. H. A. and Ngah, N. 2021. A brief review on the thiazole derivatives: Synthesis methods and biological activities. Malaysian Journal of Analytical Sciences, 25: 257-267.

Rouf, A. and Tanyeli, C. 2015. Bioactive thiazole and benzothiazole derivatives. European Journal of Medicinal Chemistry, 97: 911-927.

Santos, J. C., Andres, J., Aizman, A. and Fuentealba, P. 2005. An aromaticity scale based on the topological analysis of the electron localization function including σ and π contributions. Journal of Chemical Theory and Computation, 1(1): 83-86.

Sauer, A. C., Leal, J. G., Stefanello, S. T., Leite, M. T., Souza, M. B., Soares, F. A. and Dornelles, L. 2017. Synthesis and antioxidant properties of organosulfur and organoselenium compounds derived from 5-substituted-1, 3, 4-oxadiazole/thiadiazole-2-thiols. Tetrahedron Letters, 58(1): 87-91.

Seriy, S. 2015. Modern Ab-Initio calculations on modified Tomas-Fermi-Dirac theory. Open Journal of Modelling and Simulation, 3(3): 96.

Sherrill, C. D. 2002. Introduction to electronic structure theory. Georgia Institute of Technology, 1-10.

Sholl, D. S. and Steckel, J. A. 2022. Density functional theory: a practical introduction. John Wiley & Sons, 224 page, New York.

Siddiqui, N., Arshad, M. F., Ahsan, W. and Alam, M. S. 2009. Thiazoles: a valuable insight into the recent advances and biological activities. International Journal of Pharmaceutical Sciences and Drug Research, 1(3): 136-143.

Springborg, M. 2000. Methods of electronic-structure calculations: From molecules to solids. Reports on Progress in Physics, 75(3): 036503.

Svishcheva, G. R., Belonogova, N. M. and Axenovich, T. I. 2015. Region-based association test for familial data under functional linear models. PloS One, 10(6): e0128999.

Thomas, L. H. 1926. The motion of the spinning electron. Nature, 117(2945): 514-514.

Traube, F. R. and Carell, T. 2017. The chemistries and consequences of DNA and RNA methylation and demethylation. RNA Biology, 14(9): 1099-1107.

Udhayakala, P. and Rajendiran, T. V. 2011. Computational investigations on the corrosion inhibition efficiency of some pyridine based alkaloids. Journal of Chemical, Biological and Physical Sciences, 2(1): 172.

Valone, S. M. 2010. Quantal density functional theory II. Approximation methods and applications. Journal of the American Chemical Society, 132(32): 11387-11388.

Van Der Kolk, M. R., Janssen, M. A., Rutjes, F. P. and Blanco-Ania, D. 2022. Cyclobutanes in small-molecule drug candidates. ChemMedChem, 17(9): e202200020.

Wang, D. and Lippard, S. J. 2005. Cellular processing of platinum anticancer drugs. Nature Reviews Drug Discovery, 4(4): 307-320.

Willstätter, R. and Bruce, J. 1907. Zur Kenntnis der Cyclobutanreihe. Berichte der Deutschen Chemischen Gesellschaft, 40(4): 3979-3999.

Young, D. 2004. Computational chemistry: A practical guide for applying techniques to real world problems. John Wiley & Sons, 408 page, New York.

Yurttaş, L., Özkay, Y., Karaca Gençer, H. and Acar, U. 2015. Synthesis of some new thiazole derivatives and their biological activity evaluation. Journal of Chemistry, 2015.

Zamigajlo, L. L., Vinnyk, A. O., Turov, O. V. and Kolos, N. M. 2013. A new approach to 2, 4, 5 trisubstituted thiazoles from β dicarbonylic compounds, arylglyoxals and thioamides. Ukrainica Bioorganica Acta, 1: 37-43.